



## Journal of Prime Research in Mathematics



# A Novel Approach for the Visualization of Constrained Data using $GC^1$ Bi-Cubic Functions

Farheen Ibraheem<sup>a,\*</sup>, Ayesha Shakeel<sup>b</sup>, Muhammad Bilal Riaz<sup>c</sup>

<sup>a</sup>Department of Mathematics, Forman Christian College-A Chartered University-FCCU, Lahore, Pakistan.

<sup>b</sup>Department of Mathematics, University of Wah, Wah Cantt, Pakistan.

<sup>c</sup>Department of Mathematics, University of the Management and Technology- UMT, Lahore, Pakistan.

---

## Abstract

One of the fundamental issues in engineering, computer graphics, data visualization, interpolation and many more areas is to create a shape preserving surface from supplied data points. Data can be characterized as convex, monotone and positive. This research focuses on developing new smooth and efficient shape preserving schemes for convex, monotone and positive 3D data set positioned on a rectangular mesh. For this purpose, a  $GC^1$  continuous cubic function with two free parameters have been advanced to  $GC^1$  bi-cubic coons surface patches. There are eight free shape parameters in each rectangular patch which are constrained to ascertain these intrinsic data attributes that is convexity, positivity and monotonicity. The proposed interpolant governs the shape of data locally and data dependent constraints on shape parameters manage the shape preservation. Moreover, proposed scheme is verified and demonstrated graphically.

**Keywords:** Shape preservation, rational function, convex curve and surface,  $GC^1$  continuity .  
**2010 MSC:** 65D05, 65D07.

---

## 1. Introduction and Preliminaries

Shape preservation plays a vital role in countless fields such as medical imaging, computer graphics, reverse engineering, automotive, video gaming, object designing, aerospace industries and atmospheric science. Demographic inflation, measure of downpour, distribution of probability, volumetric mass of a substance, height of a person are some examples where data values are always positive. Monotone data arise from phenomenon such as empirical option pricing model in finance [2], hemoglobin level in blood, age of a person over time and credit card screening application. Convexity, another prime characteristic of data is visible in problems like non linear programming, optimal control and architecture. Shape conserving interpolation

---

\*Corresponding author

Email addresses: [farheenibraheem@fcccollege.edu.pk](mailto:farheenibraheem@fcccollege.edu.pk) (Farheen Ibraheem), [ayesha.shakeel@uow.edu.pk](mailto:ayesha.shakeel@uow.edu.pk) (Ayesha Shakeel), [bilal.riaz@umt.edu.pk](mailto:bilal.riaz@umt.edu.pk) (Muhammad Bilal Riaz)

Received : 28 April 2022; Accepted: 01 September 2022; Published Online: 03 October 2022.

refers to interpolating schemes that mimics the intrinsic attribute of data in visual display. Thus, it is indispensable to formulate computationally efficient and attractive visualizations for data stemming from different scientific phenomena or mathematical functions.

Shape-preserving techniques are also extensively employed in a wide variety of domains, including robotics, chemical processes, and software design for machines. A lathe is used to create ornaments, cut wood for wooden furniture, make ceramics, and other things. Use of shape-preserving software is required for the lathe path design. The robots' paths are planned using shape-preserving interpolation methods, which are also used in chemistry. For PARFAC modelling of the fluorescence data, they are employed in chemistry. Applications for signal processing, manipulating photogrammetric data, etc. are more numerous.

Shape preserving interpolation of convex, positive and monotone data has been researched by several authors [1]- [20] in recent past. Duan et al. [13] investigated a method called point-control for reshaping the interpolating surfaces by choosing appropriate properties of bivariate rational cubic spline such that the interpolation data is not altered. Han [20] established  $C^1$  piecewise function of the form quartic/quadratic and put constraints on shape parameters in its description. Hussain and Bashir [5] suggested a rational,  $C^1$  bi-cubic shape-preserving algorithm to retain the positive and monotone form of the 3D data. Data dependent constraints are developed to withhold the shape of the monotone, constrained and positive data given on rectangular grids. Hussain et al. [10] advanced geometric  $C^1$  continuous, quadratic trigonometric functions to bi cubic partially blended function, comprises of four free parameters. Hussain et al. [4] presented  $C^1$ , local rational bi-cubic interpolating function with eight free parameters for conserving the positive, monotone and convex forms of surface data. Data dependent constraints are implemented among four of these parameters. The remaining are the uncontrolled ones, hence free to acquire the smoothest surface. Sarfraz and Hussain [9] designed a smoother piecewise rational cubic function to retain the positive, monotone and convex features of data. Sarfraz et al. [8] contributed in developing a piecewise rational cubic function which is constructed with the aid of four free parameters in each of its interval. The resulting 2D data is graphically displayed. The authors used four free parameter; two for conserving geometric feature of data while two were set free for the enhancement of the interpolating curves. Sarfraz et al. [7] focused on evolving a novel curve interpolation scheme and visualized the data configured. The authors proposed schemes to preserve convexity, positivity and monotonicity of the intrinsic shaped data. Also, a strategy for the data lying above the line for shape preservation was introduced. This paper extends the work done by Hussain et al. [2], in which authors have constructed a  $GC^1$  cubic interpolant consisting of two free parameters in Ball form. In [2], authors had put forth three schemes through which the shapes of positive, monotone and convex 2D data was preserved by adding constraints to the free parameters. This article further builds up the positivity, monotonicity and convexity preserving schemes to interpolate 3D positive data, 3D monotone data and 3D convex data respectively. The proposed interpolating technique has a unique degree on each rectangular mesh.

The proposed algorithm has been compared with existing schemes in literature and its advantages are as follows:

- Positive and monotone shape of 3D regular data is preserved in [19] by developing conditions on partial derivatives which fails to retain the inherent shape of data with derivatives. The proposed  $GC^1$  scheme can be applied to both data with derivatives and data as it restricts parameters for shape preservation.
- The monotonicity preserving scheme in [12] derive constraints on the degree of the interpolating function whereas the proposed scheme are of unique degree for the entire domain.
- In [5] and [11], shape conserving techniques were rational but the proposed schemes here in this paper are integral and less expensive computationally. Comparative analysis of CPU time is encapsulated in Table 1

Table 1: Comparative Analysis of CPU Time

Case	Proposed Schemes	[10]	[5]	[11]
Example 1	0.87s	0.9600s	1.0700s	1.1632s
Example 2	0.97s	1.1832s	1.2300s	1.4130s
Example 3	1.132s	1.232s	1.324s	1.433s

- The proposed shape preserving  $GC^1$  interpolation schemes are local.

The paper is carried forward in such a manner that Section 2 reviews the geometric  $C^1(GC^1)$  continuous function of cubic form [2]. This function [2] is advanced to geometric  $C^1$  continuous partially blended bi-cubic function positioned on a rectangular grid in Section 3. Moreover, shape preserving constraints have also been developed in this section. Section 4 exhibits verification of suggested algorithm with the help of few examples. Finally, Section 5 summarizes the research work and completes the paper.

## 2. $GC^1$ Continuous Cubic Function

Let  $\zeta_1 = \varrho_0 < \varrho_1 < \varrho_2 < \dots < \varrho_n = \zeta_2$  be the partition of the interval  $[\zeta_1, \zeta_2]$  for the set of data points  $\{(\varrho_i, \sigma_i), i = 0, 1, \dots, n\}$ . The piecewise  $GC^1$  continuous cubic function [2] involving two free parameters  $\alpha_i$  and  $\beta_i$  is specified on each subinterval  $[\varrho_i, \varrho_{i+1}]$ ,  $i = 0, 1, \dots, n-1$  as

$$\mathcal{S}(\varrho) \equiv \mathcal{S}_i(\varrho) = \hat{A}_0(1-\theta)^2 + \hat{A}_1(1-\theta)^2\theta + \hat{A}_2(1-\theta)\theta^2 + \hat{A}_3\theta^2, \quad (1)$$

where

$$\hat{A}_0 = \sigma_i, \hat{A}_1 = 2\sigma_i + \frac{h_i \tilde{d}_i}{\alpha_i}, \hat{A}_2 = 2\sigma_{i+1} - \frac{h_i \tilde{d}_{i+1}}{\beta_i}, \hat{A}_3 = \sigma_{i+1},$$

$h_i = \varrho_{i+1} - \varrho_i$ ,  $\theta = \frac{\varrho - \varrho_i}{h_i}$ . The free parameters  $\alpha_i$  and  $\beta_i$  are assumed positive real numbers. The  $GC^1$  cubic interpolant (1) has the following properties:

$$\begin{aligned} S(\varrho_i) &= \sigma_i, \quad S(\varrho_{i+1}) = \sigma_{i+1}, \\ S^{(1)}(\varrho_i) &= \frac{\tilde{d}_i}{\alpha_i}, \quad S^{(1)}(\varrho_{i+1}) = \frac{\tilde{d}_{i+1}}{\beta_i}. \end{aligned}$$

Here  $S^{(1)} = \frac{dS}{d\varrho}$  and  $\tilde{d}_i$  denotes the derivatives at knots  $\varrho_i$ . It is to be noted that when  $\alpha_i = 1$  and  $\beta_i = 1$ , the cubic function (1) reduces to Cubic Hermite Spline.

## 3. Bi-Cubic Coons Surface Patch

The piecewise  $GC^1$  Cubic Function [2] is advanced to the Bi-cubic  $GC^1$  Function  $\mathcal{S}(\varrho, \sigma)$  over rectangular domain  $\mathcal{D} = [\varrho_0, \varrho_m] \times [\sigma_0, \sigma_n]$ .

Let  $\{(\varrho_k, \sigma_l, Z_{k,l}); k = 0, 1, 2, \dots, m, l = 0, 1, 2, \dots, n\}$  be 3D data set positioned over a rectangular mesh and  $\omega: \zeta_1 = \varrho_0 < \varrho_1 < \dots < \varrho_m = \zeta_2$  be segregation of  $[\zeta_1, \zeta_2]$

and  $\hat{\omega}: \xi_1 = \rho_0 < \rho_1 < \dots < \rho_n = \xi_2$  be segregation of  $[\xi_1, \xi_2]$

A Bi-Cubic  $GC^1$  Function is positioned on a rectangular region  $\mathcal{R}_{i,j} = [\varrho_k, \varrho_{k+1}] \times [\sigma_l, \sigma_{l+1}]$ ;  $k = \{0, 1, \dots, m-1\}$ ,  $l = \{0, 1, \dots, n-1\}$  as:

$$\mathcal{S}(\varrho, \sigma) = -\mathcal{A}F\mathcal{B}^T, \quad (2)$$

$$\text{where } F = \begin{bmatrix} 0 & \mathcal{S}(\varrho, \sigma_l) & \mathcal{S}(\varrho, \sigma_{l+1}) \\ \mathcal{S}(\varrho_k, \sigma) & \mathcal{S}(\varrho_k, \sigma_l) & \mathcal{S}(\varrho_k, \sigma_{l+1}) \\ \mathcal{S}(\varrho_{k+1}, \sigma) & \mathcal{S}(\varrho_{k+1}, \sigma_l) & \mathcal{S}(\varrho_{k+1}, \sigma_{l+1}) \end{bmatrix},$$

$$\mathcal{A} = \begin{bmatrix} -1 & \in_{0,3}^k(\varrho) & \in_{3,3}^k(\varrho) \end{bmatrix},$$

$$\mathcal{B} = \begin{bmatrix} -1 & \in_{0,3}^l(\sigma) & \in_{3,3}^l(\sigma) \end{bmatrix},$$

$\in_{0,3}^k(\varrho)$ ,  $\in_{3,3}^k(\varrho)$ ,  $\in_{0,3}^l(\sigma)$  and  $\in_{3,3}^l(\sigma)$  are cubic Hermite blending functions.  
On the boundary of each rectangular patch,

$$\mathcal{R}_{i,j} = [\varrho_k, \varrho_{k+1}] \times [\sigma_l, \sigma_{l+1}],$$

GC<sup>1</sup>Cubic Functions (2) are defined as  $\mathcal{S}(\varrho, \sigma_l)$ ,  $\mathcal{S}(\varrho, \sigma_{l+1})$ ,  $\mathcal{S}(\varrho_k, \sigma)$  and  $\mathcal{S}(\varrho_{k+1}, \sigma)$ .  
where

$$\mathcal{S}(\varrho, \sigma_l) = \mu_0(1 - \theta)^2 + \mu_1(1 - \theta)^2\theta + \mu_2(1 - \theta)\theta^2 + \mu_3\theta^2, \quad (3)$$

and

$$\begin{aligned} \mu_0 &= Z_{k,l}, \\ \mu_1 &= 2Z_{k,l} + \frac{h_k Z_{k,l}^\varrho}{\alpha_{i,j}}, \\ \mu_2 &= 2Z_{k+1,l} - \frac{h_k Z_{k+1,l}^\varrho}{\beta_{k,l}}, \\ \mu_3 &= Z_{k+1,l}, \end{aligned}$$

with  $\theta = \frac{\varrho - \varrho_k}{h_k}$ ,  $h_k = \varrho_{k+1} - \varrho_k$

$$\mathcal{S}(\varrho, \sigma_{l+1}) = \delta_0(1 - \theta)^2 + \delta_1(1 - \theta)^2\theta + \delta_2(1 - \theta)\theta^2 + \delta_3\theta^2, \quad (4)$$

and

$$\begin{aligned} \delta_0 &= Z_{k,l+1}, \\ \delta_1 &= 2Z_{k,l+1} + \frac{h_k Z_{k,l+1}^\varrho}{\alpha_{k,l+1}}, \\ \delta_2 &= 2Z_{k+1,l+1} - \frac{h_k F_{k+1,l+1}^\varrho}{\beta_{k,l+1}}, \\ \delta_3 &= Z_{k+1,l+1}, \end{aligned}$$

$$\mathcal{S}(\varrho_k, \sigma) = \tau_0(1 - \phi)^2 + \tau_1(1 - \phi)^2\phi + \tau_2(1 - \phi)\phi^2 + \tau_3\phi^2, \quad (5)$$

and

$$\begin{aligned} \tau_0 &= Z_{k,l}, \\ \tau_1 &= 2Z_{k,l} + \frac{\hat{h}_l Z_{k,l}^\sigma}{\hat{\alpha}_{k,l}}, \\ \tau_2 &= 2Z_{k,l+1} - \frac{\hat{h}_l Z_{k,l+1}^\sigma}{\hat{\beta}_{k,l}}, \\ \tau_3 &= Z_{k,l+1}, \end{aligned}$$

with  $\phi = \frac{\sigma - \sigma_l}{\hat{h}_l}$ ,  $\hat{h}_l = \sigma_{l+1} - \sigma_l$

$$\mathcal{S}(\varrho_{k+1}, \sigma) = \omega_0 (1 - \phi)^2 + \omega_1 (1 - \phi)^2 \phi + \omega_2 (1 - \phi) \phi^2 + \omega_3 \phi^2, \quad (6)$$

and

$$\begin{aligned} \omega_0 &= Z_{k+1,l}, \\ \omega_1 &= 2Z_{k+1,l} + \frac{\hat{h}_l Z_{k+1,l}^\sigma}{\hat{\alpha}_{k+1,l}}, \\ \omega_2 &= 2Z_{k+1,l+1} - \frac{\hat{h}_l Z_{k+1,l+1}^\sigma}{\hat{\beta}_{k+1,l}}, \\ \omega_3 &= Z_{k+1,l+1}, \end{aligned}$$

### 3.1. Positivity Preserving $GC^1$ Surface

Let  $\{(\varrho_k, \sigma_l, Z_{k,l}), k = \{0, 1, \dots, m\}, l = \{0, 1, \dots, n\}\}$  be the set of given positive data points described over rectangular patch

$$\begin{aligned} \mathcal{R}_{i,j} &= [\varrho_k, \varrho_{k+1}] \times [\sigma_l, \sigma_{l+1}]; k = \{0, 1 \dots m-1\}, l = \{0, 1, \dots n-1\}, \\ &\text{such that } Z_{k,l} > 0, \forall k, l. \end{aligned}$$

The  $GC^1$  Bi-cubic surface (2) preserves positivity if the boundary curves  $\mathcal{S}(\varrho, \sigma_l)$ ,  $\mathcal{S}(\varrho, \sigma_{l+1})$ ,  $\mathcal{S}(\varrho_k, \sigma)$  and  $\mathcal{S}(\varrho_{k+1}, \sigma)$  defined in (3), (4), (5) and (6) are positive.

Now,  $\mathcal{S}(\varrho, \sigma_l) > 0$  if  $\varphi_0 (1 - \theta)^2 + \varphi_1 (1 - \theta)^2 \theta + \varphi_2 (1 - \theta) \theta^2 + \varphi_3 \theta^2 > 0$ ,

which is realizable if  $\varphi_0, \varphi_1, \varphi_2, \varphi_3$  are all positive and this yields the following constraints on free parameter  $\alpha_{k,l} > -\frac{h_k Z_{k,l}^\varrho}{2Z_{k,l}}$  and  $\beta_{k,l} > \frac{h_k Z_{k+1,l}^\varrho}{2Z_{k+1,l}}$  where  $h_k = \varrho_{k+1} - \varrho_k$

Also,  $\mathcal{S}(\varrho, \sigma_{l+1}) > 0$  if  $\delta_0 (1 - \theta)^2 + \delta_1 (1 - \theta)^2 \theta + \delta_2 (1 - \theta) \theta^2 + \delta_3 \theta^2 > 0$ ,

which is possible if  $\delta_0, \delta_1, \delta_2, \delta_3$  are all positive and this confers the following condition

$$\alpha_{k,l+1} > -\frac{h_k Z_{k,l+1}^\varrho}{2Z_{k,l+1}} \text{ and } \beta_{i,j+1} > \frac{h_k Z_{k+1,l+1}^\varrho}{2Z_{k+1,l+1}}.$$

Likewise,  $\mathcal{S}(\varrho_k, \sigma) > 0$  if  $\sigma_0 (1 - \phi)^2 + \sigma_1 (1 - \phi)^2 \phi + \sigma_2 (1 - \phi) \phi^2 + \sigma_3 \phi^2 > 0$ ,

which enforces  $\sigma_0, \sigma_1, \sigma_2, \sigma_3$  to be positive and this delivers the following constraints

$$\hat{\alpha}_{i,j} > -\frac{\hat{h}_l Z_{k,l}^\sigma}{2Z_{k,l}} \text{ and } \hat{\beta}_{i,j} > \frac{\hat{h}_l Z_{k,l+1}^\sigma}{2Z_{k,l+1}}, \text{ where } \hat{h}_l = \hat{h}_{l+1} - \hat{h}_l.$$

Moreover,  $\mathcal{S}(\varrho_{k+1}, \sigma) > 0$  if  $\omega_0 (1 - \phi)^2 + \omega_1 (1 - \phi)^2 \phi + \omega_2 (1 - \phi) \phi^2 + \omega_3 \phi^2 > 0$ ,

which means  $\omega_0, \omega_1, \omega_2, \omega_3$  are all positive and this gives the following conditions

$$\hat{\alpha}_{k+1,l} > -\frac{\hat{h}_l Z_{k+1,l}^\sigma}{2Z_{k+1,l}} \text{ and } \hat{\beta}_{k+1,l} > \frac{\hat{h}_l Z_{k+1,l+1}^\sigma}{2Z_{k+1,l+1}}.$$

The content presented above can be concluded as:

**Theorem 1** The sufficient conditions for a piecewise bi-cubic function to be positive over a rectangular grid  $\mathcal{R}_{i,j} = [\varrho_k, \varrho_{k+1}] \times [\sigma_l, \sigma_{l+1}]; k = \{0, 1 \dots m-1\}, l = \{0, 1, \dots n-1\}$  in (2) are:

$$\begin{aligned} \alpha_{k,l} &> \text{Max} \left\{ 0, -\frac{h_k Z_{k,l}^\varrho}{2Z_{i,j}} \right\}, \quad \beta_{k,l} > \text{Max} \left\{ 0, \frac{h_k Z_{k+1,l}^\varrho}{2Z_{k+1,l}} \right\}, \\ \alpha_{k,l+1} &> \text{Max} \left\{ 0, -\frac{h_k Z_{k,l+1}^\varrho}{2Z_{k,l+1}} \right\}, \quad \beta_{k,l+1} > \text{Max} \left\{ 0, \frac{h_k Z_{k+1,l+1}^\varrho}{2Z_{k+1,l+1}} \right\}, \end{aligned}$$

$$\begin{aligned}\hat{\alpha}_{k,l} &> \text{Max} \left\{ 0, -\frac{\hat{h}_l Z_{k,l}^\sigma}{2Z_{k,l}} \right\}, \quad \hat{\beta}_{k,l} > \text{Max} \left\{ 0, \frac{\hat{h}_l Z_{k,l+1}^\sigma}{2Z_{k,l+1}} \right\}, \\ \hat{\alpha}_{k+1,l} &> \text{Max} \left\{ 0, -\frac{\hat{h}_l Z_{k+1,l}^\sigma}{2Z_{k+1,l}} \right\}, \quad \hat{\beta}_{k+1,l} > \text{Max} \left\{ 0, \frac{\hat{h}_l Z_{k+1,l+1}^\sigma}{2Z_{k+1,l+1}} \right\}.\end{aligned}$$

The above conditions can be rearranged as:

$$\begin{aligned}\alpha_{k,l} &= r_{k,l} + \text{Max} \left\{ 0, -\frac{h_k Z_{k,l}^\sigma}{2Z_{k,l}} \right\}, \quad r_{k,l} > 0, \quad \beta_{k,l} = s_{k,l} + \text{Max} \left\{ 0, \frac{h_k Z_{k,l+1}^\sigma}{2Z_{k,l+1}} \right\}, \quad s_{k,l} > 0, \\ \alpha_{k,l+1} &= t_{k,l} + \text{Max} \left\{ 0, -\frac{h_k Z_{k,l+1}^\sigma}{2Z_{k,l+1}} \right\}, \quad t_{k,l} > 0, \quad \beta_{k,l+1} = u_{k,l} + \text{Max} \left\{ 0, \frac{h_k Z_{k+1,l+1}^\sigma}{2Z_{k+1,l+1}} \right\}, \quad u_{k,l} > 0, \\ \hat{\alpha}_{k,l} &= \hat{r}_{k,l} + \text{Max} \left\{ 0, -\frac{\hat{h}_l Z_{k,l}^\sigma}{2Z_{k,l}} \right\}, \quad \hat{r}_{k,l} > 0, \quad \hat{\beta}_{k,l} = \hat{s}_{k,l} + \text{Max} \left\{ 0, \frac{\hat{h}_l Z_{k,l+1}^\sigma}{2Z_{k,l+1}} \right\}, \quad \hat{s}_{k,l} > 0, \\ \hat{\alpha}_{k+1,l} &= \hat{t}_{k,l} + \text{Max} \left\{ 0, -\frac{\hat{h}_l Z_{k+1,l}^\sigma}{2Z_{k+1,l}} \right\}, \quad \hat{t}_{k,l} > 0, \quad \hat{\beta}_{k+1,l} = \hat{u}_{k,l} + \text{Max} \left\{ 0, \frac{\hat{h}_l Z_{k+1,l+1}^\sigma}{2Z_{k+1,l+1}} \right\}, \quad \hat{u}_{k,l} > 0.\end{aligned}$$

### Algorithm

**Step 1.** Take the positive data set  $\{(\varrho_k, \sigma_l, Z_{k,l}), k = \{0, 1, \dots, m\}, l = \{0, 1, \dots, n\}\}$ .

**Step 2.** Estimate the derivatives  $Z_{k,l}^\sigma, Z_{k,l}^\sigma, Z_{k,l}^{\sigma\sigma}$  by arithmetic mean method.

**Step 3.** Apply Theorem 1 to calculate the values of free parameters.

**Step 4.** Substitute the data set,  $\{(\varrho_k, \sigma_l, Z_{k,l}), k = \{0, 1, \dots, m\}, l = \{0, 1, \dots, n\}\}$  and values of free parameter in (2) to interpolate and visualize positive data.

### 3.2. Monotonicity Preserving $GC^1$ Surfaces

Let  $(\varrho_k, \sigma_l, Z_{k,l}), k = 0, 1, \dots, m, l = 0, 1, \dots, n$  be the given set of monotone data points defined over rectangular patch

$$R_{k,l} = [\varrho_k, \varrho_{k+1}] \times [\sigma_l, \sigma_{l+1}]; k = \{0, 1 \dots m-1\}, l = 0, 1, \dots, n-1$$

$$\begin{aligned}s.t. & Z_{k,l} < Z_{k+1,l}, Z_{k,l} < Z_{k,l+1}, \\ & Z_{k,l}^\sigma > 0, Z_{k,l}^\sigma > 0, \\ & \Delta_{k,l} > 0, \Delta_{k,l} > 0.\end{aligned}$$

$$\text{where } \Delta_{k,l} = \frac{Z_{k+1,l} - Z_{k,l}}{h_k}, \Delta_{k,l} = \frac{Z_{k,l+1} - Z_{k,l}}{\hat{h}_l}$$

The  $GC^1$  bi-cubic surface patches (2) inherit all the properties of network of the boundary curves  $S(\varrho, \sigma_l), S(\varrho, \sigma_{l+1}), S(\varrho_k, \sigma)$  and  $S(\varrho_{k+1}, \sigma)$  defined in (7), (8), (9) and (10). The  $GC^1$  bi-cubic surface patch (2) preserves monotonicity if the boundary curves as defined are monotone.

$S(\varrho, f_j)$  is monotone if  $S^{(1)}(\varrho, \sigma_l) > 0$  i.e.

$$S^{(1)}(\varrho, \sigma_l) = \sum_{p=0}^2 \theta^p \dot{\xi}_p \quad (7)$$

where

$$\dot{\xi}_0 = \frac{Z_{k,l}^\sigma}{\alpha_{k,l}},$$

$$\dot{\xi}_1 = 6\Delta_{k,l} - 4\frac{Z_{k,l}^\sigma}{\alpha_{k,l}} - 2\frac{Z_{k+1,l}^\sigma}{\beta_{k,l}}$$

$$\dot{\xi}_2 = -6\Delta_{k,l} + 3\frac{Z_{k,l}^\varrho}{\alpha_{k,l}} + 3\frac{Z_{k+1,l}^\varrho}{\beta_{k,l}}$$

$$S^{(1)}(\varrho, \sigma_l) > 0 \quad \text{if} \\ \sum_{p=0}^2 \theta^p \dot{\xi}_p > 0$$

$$\sum_{p=0}^2 \theta^p \dot{\xi}_p > 0 \quad \text{if} \\ \dot{\xi}_p > 0, p = 0, 1, 2.$$

$$\dot{\xi}_p > 0, p = 0, 1, 2 \quad \text{if} \\ \alpha_{k,l} > \frac{Z_{k,l}^\varrho}{\Delta_{k,l}} \text{ and } \beta_{k,l} > \frac{Z_{k+1,l}^\varrho}{\Delta_{k,l}}$$

$$S(\varrho, \sigma_{l+1}) \text{ is monotone if } S^{(1)}(\varrho, \sigma_{l+1}) > 0 \text{ i.e.} \\ S^{(1)}(\varrho, \sigma_{l+1}) = \sum_{q=0}^2 \theta^q \ddot{\xi}_q \quad (8)$$

$$\text{where} \\ \ddot{\xi}_0 = \frac{F_{k,l+1}^\varrho}{\alpha_{k,l+1}},$$

$$\ddot{\xi}_1 = 6\Delta_{k,l+1} - 4\frac{Z_{k,l+1}^\varrho}{\alpha_{k,l+1}} - 2\frac{Z_{k+1,l+1}^\varrho}{\beta_{k,l+1}}$$

$$\ddot{\xi}_2 = -6\Delta_{i,j+1} + 3\frac{Z_{i,j+1}^\varrho}{\alpha_{i,j+1}} + 3\frac{Z_{i+1,j+1}^\varrho}{\beta_{i,j+1}}$$

$$S^{(1)}(\varrho, \sigma_{l+1}) > 0 \quad \text{if} \\ \sum_{q=0}^2 \theta^q \ddot{\xi}_q > 0$$

$$\sum_{q=0}^2 \theta^q \ddot{\xi}_q > 0 \quad \text{if} \\ \ddot{\xi}_q > 0, q = 0, 1, 2.$$

$$\ddot{\xi}_q > 0, q = 0, 1, 2 \text{ if} \\ \alpha_{k,l+1} > \frac{Z_{k,l+1}^\varrho}{\Delta_{k,l+1}} \text{ and } \beta_{k,l+1} > \frac{Z_{k+1,l+1}^\varrho}{\Delta_{k,l+1}}$$

$$S(\varrho_i, \sigma) \text{ is monotone if } S^{(1)}(\varrho_i, \sigma) > 0 \text{ i.e.} \\ S^{(1)}(\varrho_i, \sigma) = \sum_{r=0}^2 \varphi^r \dot{\eta}_r \quad (9)$$

$$\text{where} \\ \dot{\eta}_0 = \frac{Z_{k,l}^\sigma}{\alpha_{k,l}},$$

$$\dot{\eta}_1 = 6\Delta_{k,l} - 4\frac{Z_{k,l}^\sigma}{\alpha_{k,l}} - 2\frac{Z_{k,l+1}^\sigma}{\beta_{k,l}}$$

$$\dot{\eta}_2 = -6\Delta_{k,l} + 3\frac{Z_{k,l}^\sigma}{\alpha_{k,l}} + 3\frac{Z_{k,l+1}^\sigma}{\beta_{k,l}}$$

$$S^{(1)}(\varrho_k, \sigma) > 0 \text{ if} \\ \sum_{r=0}^2 \varphi^r \dot{\eta}_r > 0$$

$$\sum_{r=0}^2 \varphi^r \dot{\eta}_r > 0 \text{ if} \\ \dot{\eta}_r > 0, r = 0, 1, 2.$$

$$\dot{\eta}_r > 0, r = 0, 1, 2 \text{ if}$$

$$\alpha_{k,l} > \frac{F_{k,l}^\sigma}{\Delta_{k,l}} \text{ and } \beta_{k,l} > \frac{F_{k,l+1}^\sigma}{\Delta_{k,l}}$$

$$S(\varrho_{k+1}, \sigma) \text{ is monotone if } S^{(1)}(\varrho_{k+1}, \sigma) > 0 \text{ i.e.} \\ S^{(1)}(\varrho_{k+1}, \sigma) = \sum_{s=0}^2 \varphi^s \ddot{\eta}_s \quad (10)$$

$$\text{where} \\ \ddot{\eta}_0 = \frac{Z_{k+1,l}^\sigma}{\alpha_{k+1,l}},$$

$$\ddot{\eta}_1 = 6\Delta_{k+1,l} - 4\frac{Z_{k+1,l}^\sigma}{\alpha_{k+1,l}} - 2\frac{F_{k+1,l+1}^\sigma}{\beta_{k+1,l}}$$

$$\ddot{\eta}_2 = -6\Delta_{k+1,l} + 3\frac{Z_{k+1,l}^\sigma}{\alpha_{k+1,l}} + 3\frac{Z_{k+1,l+1}^\sigma}{\beta_{k+1,l}}$$

$$S^{(1)}(\varrho_{k+1}, \sigma) > 0 \text{ if} \\ \sum_{s=0}^2 \varphi^s \ddot{\eta}_s > 0$$

$$\sum_{s=0}^2 \varphi^s \ddot{\eta}_s > 0 \text{ if} \\ \ddot{\eta}_s > 0, s = 0, 1, 2.$$

$$\ddot{\eta}_s > 0, s = 0, 1, 2 \text{ if} \\ \alpha_{k+1,l} > \frac{Z_{k+1,l}^\sigma}{\Delta_{k+1,l}} \text{ and } \beta_{k+1,l} > \frac{Z_{k+1,l+1}^\sigma}{\Delta_{k+1,l}}$$

The content presented above can be stated as:

## Theorem 2

The sufficient conditions for a piecewise bi-cubic function to be monotone over a rectangular grid  $R_{k,l} = [\varrho_i, \varrho_{i+1}] \times [\sigma_i, \sigma_{j+1}]$ ;  $k = [0, 1, \dots, m-1], l = 0, 1, \dots, n-1$  in (2) are:

$$\alpha_{k,l} > \text{Max}\{0, \frac{Z_{k,l}^\sigma}{\Delta_{k,l}}\}, \beta_{k,l} > \text{Max}\{0, \frac{Z_{k+1,l}^\sigma}{\Delta_{k,l}}\} \\ \alpha_{k,l+1} > \text{Max}\{0, \frac{Z_{k,l+1}^\sigma}{\Delta_{k,l+1}}\}, \beta_{k,l+1} > \text{Max}\{0, \frac{Z_{k+1,l+1}^\sigma}{\Delta_{k,l+1}}\} \\ \alpha_{k,l} > \text{Max}\{0, \frac{Z_{k,l}^\sigma}{\Delta_{k,l}}\}, \beta_{k,l} > \text{Max}\{0, \frac{Z_{k,l+1}^\sigma}{\Delta_{k,l}}\} \\ \alpha_{k+1,l} > \text{Max}\{0, \frac{Z_{k+1,l}^\sigma}{\Delta_{k+1,l}}\}, \beta_{k+1,l} > \text{Max}\{0, \frac{Z_{k+1,l+1}^\sigma}{\Delta_{k+1,l}}\}$$

which is equivalent to following set of conditions:

$$\alpha_{k,l} = r_{k,l} + \text{Max}\{0, \frac{Z_{k,l}^\sigma}{\Delta_{k,l}}\}, r_{k,l} > 0, \beta_{k,l} = s_{k,l} + \text{Max}\{0, \frac{Z_{k+1,l}^\sigma}{\Delta_{k,l}}\}, s_{k,l} > 0, \\ \alpha_{k,l+1} = t_{k,l} + \text{Max}\{0, \frac{Z_{k,l+1}^\sigma}{\Delta_{k,l+1}}\}, t_{k,l} > 0, \beta_{k,l+1} = u_{k,l} + \text{Max}\{0, \frac{Z_{k+1,l+1}^\sigma}{\Delta_{k,l+1}}\}, u_{k,l} > 0, \\ \alpha_{k,l} = r_{k,l} + \text{Max}\{0, \frac{Z_{k,l}^\sigma}{\Delta_{k,l}}\}, r_{k,l} > 0, \beta_{k,l} = s_{k,l} + \text{Max}\{0, \frac{Z_{k,l+1}^\sigma}{\Delta_{k,l}}\}, s_{k,l} > 0, \\ \alpha_{k+1,l} = t_{k,l} + \text{Max}\{0, \frac{Z_{k+1,l}^\sigma}{\Delta_{k+1,l}}\}, t_{k,l} > 0, \beta_{k+1,l} = u_{k,l} + \text{Max}\{0, \frac{Z_{k+1,l+1}^\sigma}{\Delta_{k+1,l}}\}, u_{k,l} > 0.$$

## Algorithm

**Step 1.** Take the monotone data set  $\{(\varrho_k, \sigma_l, Z_{k,l}), k = \{0, 1, \dots, m\}, l = \{0, 1, \dots, n\}\}$ .

**Step 2.** Estimate the derivatives  $Z_{k,l}^\sigma, Z_{k,l}^\sigma, Z_{k,l}^{\sigma\sigma}$  by arithmetic mean method.

**Step 3.** Apply Theorem 2 to calculate the values of free parameters.

**Step 4.** Substitute the data set,  $\{(\varrho_k, \sigma_l, Z_{k,l}), k = \{0, 1, \dots, m\}, l = \{0, 1, \dots, n\}\}$  and values of free parameter in (2) visualize monotone surface stemming from monotone data.



### 3.3. Convexity Preserving $GC^1$ Surfaces

Let  $(\varrho_k, \sigma_l, Z_{k,l}), k = 0, 1, \dots, m, l = 0, 1, \dots, n$  be the given set of convex data points defined over rectangular patch

$$R_{k,l} = [\varrho_k, \varrho_{k+1}] \times [\sigma_l, \sigma_{l+1}]; k = \{0, 1 \dots m-1\}, l = 0, 1, \dots, n-1 \text{ such that}$$

$$Z_{k,l}^\varrho < \Delta_{k,l} < Z_{k+1,l}^\varrho, Z_{k,l+1}^\varrho < \Delta_{k,l+1} < Z_{k+1,l+1}^\varrho, \Delta_{k,l} < \Delta_{k+1,l}$$

$$Z_{k,l}^\sigma < \hat{\Delta}_{k,l} < Z_{k,l+1}^\sigma, Z_{k+1,l}^\sigma < \hat{\Delta}_{k+1,l} < Z_{k+1,l+1}^\sigma, \hat{\Delta}_{k,l} < \hat{\Delta}_{k,l+1}$$

where

$$\Delta_{k,l} = \frac{Z_{k+1,l} - Z_{k,l}}{h_i}, \hat{\Delta}_{k,l+1} = \frac{Z_{k+1,l+1} - Z_{k,l+1}}{h_i}$$

$$h_k = \varrho_{k+1} - \varrho_k, \hat{h}_l = \sigma_{l+1} - \sigma_l.$$

The  $GC^1$  bi-cubic surface patches (2) inherit all the properties of network of the boundary curves  $S(\varrho, \sigma_l)$ ,  $S(\varrho, \sigma_{l+1})$ ,  $S(\varrho_k, \sigma)$  and  $S(\varrho_{k+1}, \sigma)$  defined in (11), (12), (13) and (14). The  $GC^1$  bi-cubic surface patch (2) preserves convexity if the boundary curves as defined are convex.

$S(\varrho, \sigma_l)$  is convex if  $S^{(2)}(\varrho, \sigma_l) > 0$  i.e.

$$S^{(2)}(\varrho, \sigma_l) = 2\Theta\dot{\mu}_1 + \dot{\mu}_0 \quad (11)$$

where

$$\dot{\mu}_0 = 6\Delta_{k,l} - 4\frac{Z_{k,l}^\varrho}{\alpha_{k,l}} - 2\frac{Z_{k+1,l}^\varrho}{\beta_{k,l}}, \dot{\mu}_1 = -6\Delta_{k,l} + 3\frac{Z_{k,l}^\varrho}{\alpha_{k,l}} + 3\frac{Z_{k+1,l}^\varrho}{\beta_{k,l}}$$

$$S^{(2)}(\varrho, \sigma_l) > 0 \text{ if}$$

$$2\Theta\dot{\mu}_1 + \dot{\mu}_0 > 0$$

For this  $\dot{\mu}_1, \dot{\mu}_0 > 0$  and this imposes following constraints

$$\alpha_{k,l} > \frac{Z_{k,l}^\varrho + Z_{k+1,l}^\varrho}{2\Delta_{k,l}}, \beta_{k,l} > \frac{Z_{k,l}^\varrho + Z_{k+1,l}^\varrho}{2\Delta_{k,l}}$$

$S(\varrho, \sigma_{j+1})$  is convex if  $S^{(2)}(\varrho, \sigma_{l+1}) > 0$  i.e.

$$S^2(\varrho, \sigma_{l+1}) = 2\Theta\nu_1 + \nu_0 \quad (12)$$

where

$$\nu_0 = 6\Delta_{k,l+1} - 4\frac{Z_{k,l+1}^\varrho}{\alpha_{k,l+1}} - 2\frac{Z_{k+1,l+1}^\varrho}{\beta_{k,l+1}}, \nu_1 = -6\Delta_{k,l+1} + 3\frac{Z_{k,l+1}^\varrho}{\alpha_{k,l+1}} + 3\frac{Z_{k+1,l+1}^\varrho}{\beta_{k,l+1}}$$

$$\text{Now, } S^{(2)}(\varrho, \sigma_{l+1}) > 0 \text{ if}$$

$$2\Theta\nu_1 + \nu_0 > 0$$

and  $2\Theta\nu_1 + \nu_0 > 0$  if  $\nu_0, \nu_1 > 0$ , this results following

$$\alpha_{k,l+1} > \frac{Z_{k,l+1}^\varrho + Z_{k+1,l+1}^\varrho}{2\Delta_{k,l+1}}, \beta_{k,l+1} > \frac{Z_{k,l+1}^\varrho + Z_{k+1,l+1}^\varrho}{2\Delta_{k,l+1}}$$

$S(\varrho_k, \sigma)$  is convex if  $S^{(2)}(\varrho_k, \sigma) > 0$  i.e.

$$S^{(2)}(\varrho_k, \sigma) = 2\Theta\gamma_1 + \gamma_0 \quad (13)$$

where

$$\gamma_0 = 6\Delta_{k,l} - 4\frac{Z_{k,l}^\sigma}{\alpha_{k,l}} - 2\frac{Z_{k,l+1}^\sigma}{\beta_{k,l}}, \gamma_1 = -6\Delta_{k,l} + 3\frac{Z_{k,l}^\sigma}{\alpha_{k,l}} + 3\frac{Z_{k,l+1}^\sigma}{\beta_{k,l}}$$

$$S^{(2)}(\varrho_k, \sigma) > 0 \text{ if } 2\Theta\gamma_1 + \gamma_0 > 0 \text{ and this implies } \gamma_1, \gamma_0 > 0.$$

$$\text{Consequently, } \alpha_{k,l} > \frac{Z_{k,l}^\sigma + Z_{k,l+1}^\sigma}{2\Delta_{k,l}}, \beta_{k,l} > \frac{Z_{k,l}^\sigma + Z_{k,l+1}^\sigma}{2\Delta_{k,l}}.$$

$S(\varrho_{k+1}, \sigma)$  is convex if  $S^{(2)}(\varrho_{k+1}, \sigma) > 0$  i.e.

$$S^{(2)}(\varrho_{k+1}, \sigma) = 2\Theta\lambda_1 + \lambda_0 > 0 \quad (14)$$

where  $\lambda_0 = 6\Delta_{k+1,l} - 4\frac{Z_{k+1,l}^\sigma}{\alpha_{k+1,l}} - 2\frac{Z_{k+1,l+1}^\sigma}{\beta_{k+1,l}}$ ,  $\lambda_1 = -6\Delta_{k+1,l} + 3\frac{Z_{k+1,l}^\sigma}{\alpha_{k+1,l}} + 3\frac{Z_{k+1,l+1}^\sigma}{\beta_{k+1,l}}$   
 thus,  $\alpha_{k+1,l} > \frac{Z_{k+1,l}^\sigma + Z_{k+1,l+1}^\sigma}{2\Delta_{k+1,l}}$ ,  $\beta_{k+1,l} > \frac{F_{k+1,l}^\sigma + F_{k+1,l+1}^\sigma}{2\Delta_{k+1,l}}$

The above discussion can be briefed as:

### Theorem 3

The sufficient conditions for a piecewise bi-cubic function to be convex over a rectangular grid  $R_{k,l} = [\varrho_k, \varrho_{k+1}] \times [\sigma_l, \sigma_{l+1}]$ ;  $k = [0, 1, \dots, m-1]$ ,  $l = [0, 1, \dots, n-1]$  in (2) are:

$$\begin{aligned} \alpha_{k,l} &> \text{Max}\{0, \frac{Z_{k,l}^\varrho + F_{k+1,l}^\varrho}{2\Delta_{k,l}}\}, \beta_{k,l} > \text{Max}\{0, \frac{F_{k,l}^\varrho + F_{k+1,l}^\varrho}{2\Delta_{k,l}}\}, \Delta_{k,l} \neq 0, \\ \alpha_{k,l+1} &> \text{Max}\{0, \frac{Z_{k,l+1}^\varrho + Z_{k+1,l+1}^\varrho}{2\Delta_{k,l+1}}\}, \beta_{k,l+1} > \text{Max}\{0, \frac{Z_{k,l+1}^\varrho + Z_{k+1,l+1}^\varrho}{2\Delta_{k,l+1}}\}, \Delta_{k,l+1} \neq 0. \\ \alpha_{k,l} &> \text{Max}\{0, \frac{Z_{k,l}^\sigma + F_{k+1,l}^\sigma}{2\Delta_{k,l}}\}, \beta_{k,l} > \text{Max}\{0, \frac{Z_{k,l}^\sigma + Z_{k+1,l}^\sigma}{2\Delta_{k,l}}\}, \Delta_{k,l} \neq 0. \\ \alpha_{k+1,l} &> \text{Max}\{0, \frac{Z_{k+1,l}^\sigma + Z_{k+1,l+1}^\sigma}{2\Delta_{k+1,l}}\}, \beta_{k+1,l} > \text{Max}\{0, \frac{F_{k+1,l}^\sigma + F_{k+1,l+1}^\sigma}{2\Delta_{k+1,l}}\}, \Delta_{k+1,l} \neq 0. \end{aligned}$$

Equivalently,

$$\begin{aligned} \alpha_{k,l} &= \dot{r}_{k,l} + \text{Max}\{0, \frac{Z_{k,l}^\varrho + F_{k+1,l}^\varrho}{2\Delta_{k,l}}\}, \beta_{k,l} = \dot{s}_{k,l} + \text{Max}\{0, \frac{F_{k,l}^\varrho + F_{k+1,l}^\varrho}{2\Delta_{k,l}}\}, \\ \alpha_{k,l+1} &= \dot{t}_{k,l} + \text{Max}\{0, \frac{Z_{k,l+1}^\varrho + Z_{k+1,l+1}^\varrho}{2\Delta_{k,l+1}}\}, \beta_{k,l+1} = \dot{u}_{k,l} + \text{Max}\{0, \frac{Z_{k,l+1}^\varrho + Z_{k+1,l+1}^\varrho}{2\Delta_{k,l+1}}\}, \\ \alpha_{k,l} &= r_{k,l} + \text{Max}\{0, \frac{Z_{k,l}^\sigma + F_{k+1,l}^\sigma}{2\Delta_{k,l}}\}, \beta_{k,l} = s_{k,l} + \text{Max}\{0, \frac{Z_{k,l}^\sigma + Z_{k+1,l}^\sigma}{2\Delta_{k,l}}\}, \\ \alpha_{k+1,l} &= t_{k,l} + \text{Max}\{\frac{Z_{k+1,l}^\sigma + Z_{k+1,l+1}^\sigma}{2\Delta_{k+1,l}}\}, \beta_{k+1,l} = u_{k,l} + \text{Max}\{\frac{F_{k+1,l}^\sigma + F_{k+1,l+1}^\sigma}{2\Delta_{k+1,l}}\}. \end{aligned}$$

where  $\dot{r}_{k,l}, \dot{s}_{k,l}, \dot{t}_{k,l}, \dot{u}_{k,l}, r_{k,l}, s_{k,l}, t_{k,l}, u_{k,l} > 0$ , and  $\Delta_{k,l}, \Delta_{k,l+1}, \Delta_{k,l}, \Delta_{k+1,l} \neq 0$ .

### Algorithm

**Step 1.** Take the convex data set  $\{(\varrho_k, \sigma_l, Z_{k,l}), k = \{0, 1, \dots, m\}, l = \{0, 1, \dots, n\}\}$ .

**Step 2.** Estimate the derivatives  $Z_{k,l}^\varrho, Z_{k,l}^\sigma, Z_{k,l}^{\varrho\sigma}$  by arithmetic mean method.

**Step 3.** Apply Theorem 3 to calculate the values of free parameters.

**Step 4.** Substitute the data set,  $\{(\varrho_k, \sigma_l, Z_{k,l}), k = \{0, 1, \dots, m\}, l = \{0, 1, \dots, n\}\}$  and values of free parameter in (2) visualize monotone surface stemming from monotone data.

## 4. Numerical Example

**Example 1.** The positive function:

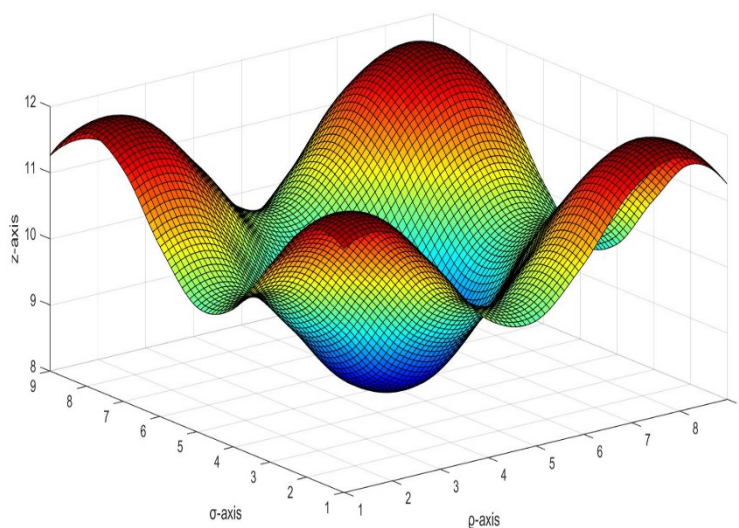
$$F(\varrho, \sigma) = \frac{\varrho\sigma(\varrho^2 - \sigma^2)}{(\varrho^2 + \sigma^2)} + 100$$

induced the positive data set, truncated to four decimal places, as shown in Table 4.1.

**Table 4.1** A positive data set

$\sigma$	$\varrho$					
	-6	-4	-2	2	4	6
-6	100.0000	109.2308	109.6000	90.4000	90.7692	100.0000
-4	90.7692	100.0000	104.8000	95.2000	100.0000	109.2308
-2	90.4000	95.2000	100.0000	100.0000	104.8000	109.6000
2	109.6000	104.8000	100.0000	100.0000	95.2000	90.4000
4	109.2308	100.0000	95.2000	104.8000	100.0000	90.7692
6	100.0000	90.7692	90.4000	109.6000	109.2308	100.0000

Adopting the scheme developed in section 3.1, Figure 1 corresponds to the positive 3D model which is produced from data set in Table 4.1. Figures 2 and 3 being the visual models of Figure 1 in  $\varrho z$  and  $\sigma z$ -planes respectively.

Figure 1: The positive  $GC^1$  Bi-cubic function.

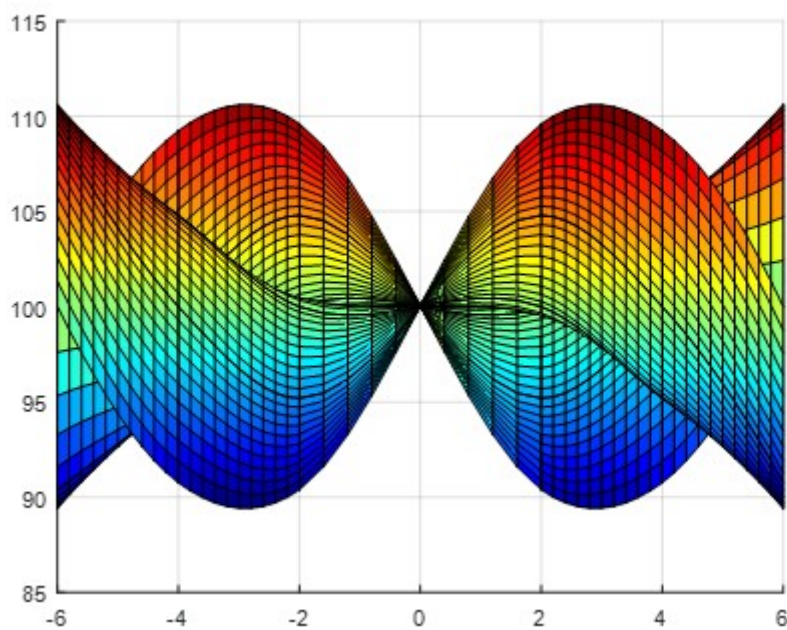


Figure 2:  $\varrho z$  view of Figure 1.

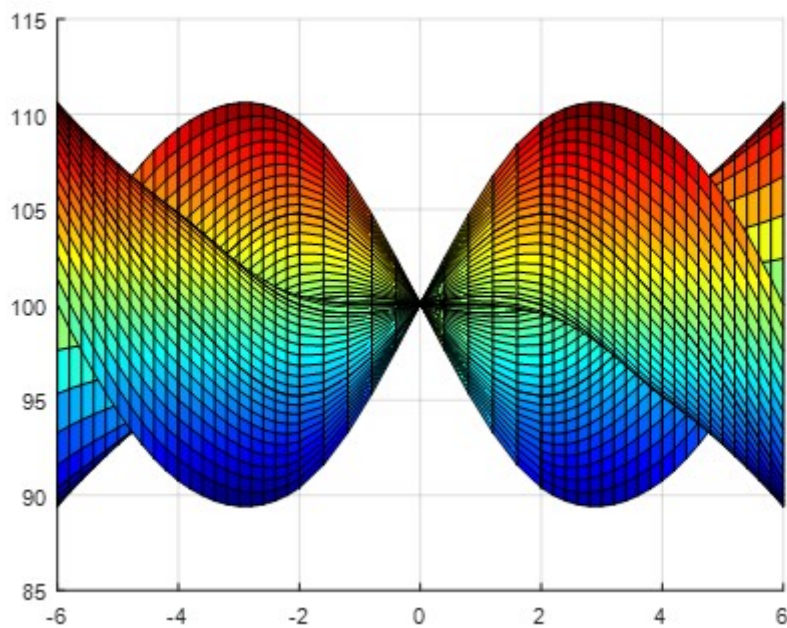


Figure 3:  $\sigma z$  view of Figure 1.

**Example 2.** The function

$$F(\varrho, \sigma) = \frac{1}{40}\varrho^2 - \frac{1}{2}\sigma + 100$$

induced the monotone data set, truncated to four decimal places, as shown in Table 4.2.

**Table 4.2** A monotone data set

$\frac{\sigma}{\varrho}$	10	20	30	40	50	60
10	97.5000	92.5000	87.5000	82.5000	77.5000	72.5000
20	105.0000	100.0000	95.0000	90.0000	85.0000	80.0000
30	117.5000	112.5000	107.5000	102.5000	97.5000	92.5000
40	135.0000	130.0000	125.0000	120.0000	115.0000	110.0000
50	157.5000	152.5000	147.5000	142.5000	137.5000	132.5000
60	185.0000	180.0000	175.0000	170.0000	165.0000	160.0000

Adopting the scheme developed in section 3.2, Figure 4 corresponds to the monotone 3D model which is produced from data set in Table 4.2. Figures 5 and 6 being the visual models of Figure 4 in  $\varrho z$  and  $\sigma z$  -planes respectively.

**Example 3.** The function

$$F(\varrho, \sigma) = \sigma^2 + 5\varrho^2 - 26$$

induced the convex data set, reduced to four decimal places, as shown in Table 4.3.

**Table 4.3** A convex data set

$\frac{\sigma}{\varrho}$	-3	-2	-1	0	1	2	3
-3	28.0000	23.0000	20.0000	19.0000	20.0000	23.0000	28.0000
-2	3.0000	-2.0000	-5.0000	-6.0000	-5.0000	-2.0000	3.0000
-1	-12.0000	-17.0000	-20.0000	-21.0000	-20.0000	-17.0000	-12.0000
0	-17.0000	-22.0000	-25.0000	-26.0000	-25.0000	-22.0000	-17.0000
1	-12.0000	-17.0000	-20.0000	-21.0000	-20.0000	-17.0000	-12.0000
2	3.0000	-2.0000	-5.0000	-6.0000	-5.0000	-2.0000	3.0000
3	28.0000	23.0000	20.0000	19.0000	20.0000	23.0000	28.0000

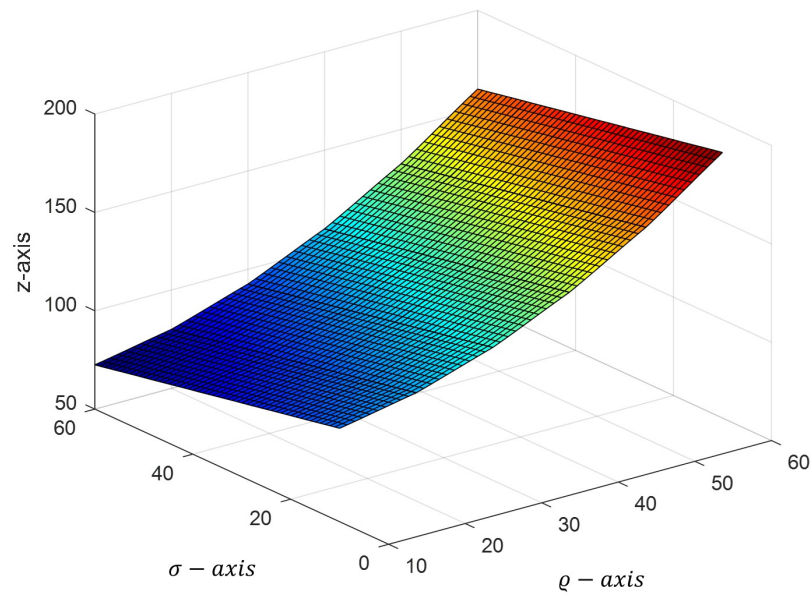


Figure 4: The monotone  $GC^1$  Bi-cubic function.

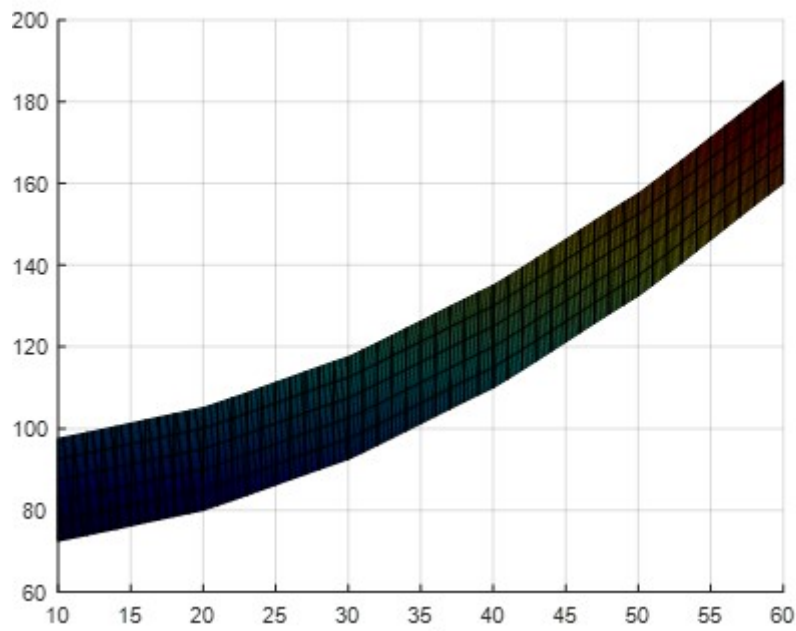


Figure 5:  $\varrho z$  view of Figure 3.



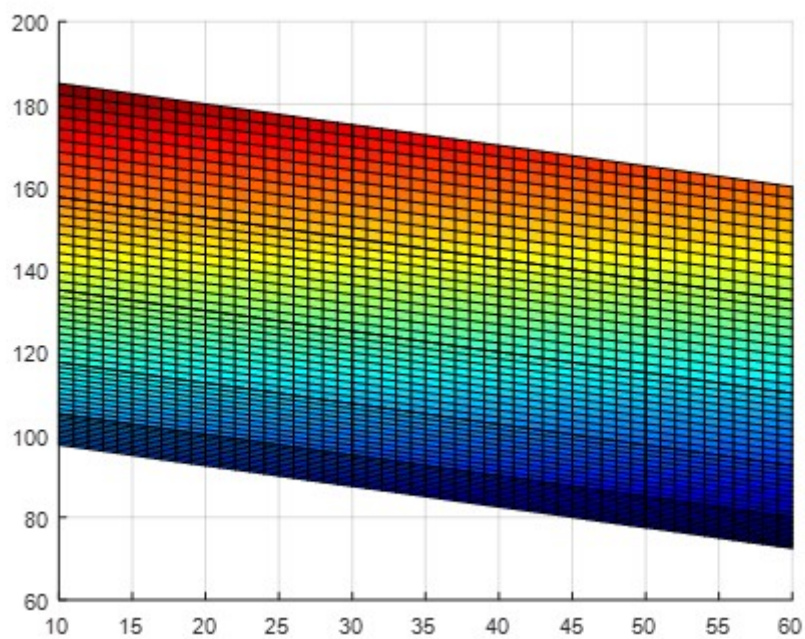


Figure 6:  $\sigma z$  view of Figure 3.

Adopting the scheme developed in section 3.3, Figure 7 corresponds to the convex 3D data in Table 4.3 is visualized. Figures 8 and 9 provide  $\rho z$  view and  $\sigma z$  view respectively.

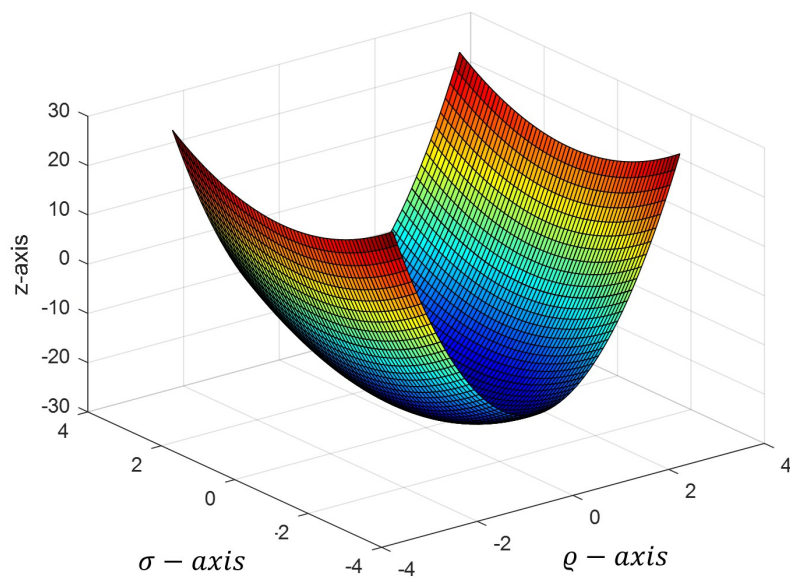


Figure 7: The convex  $GC^1$  Bi-cubic function.

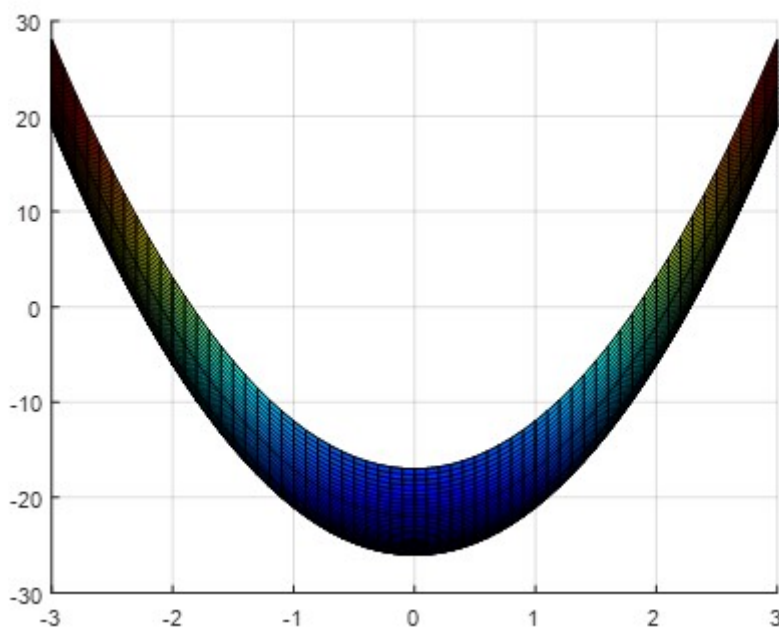


Figure 8:  $\rho z$  view of Figure 6.

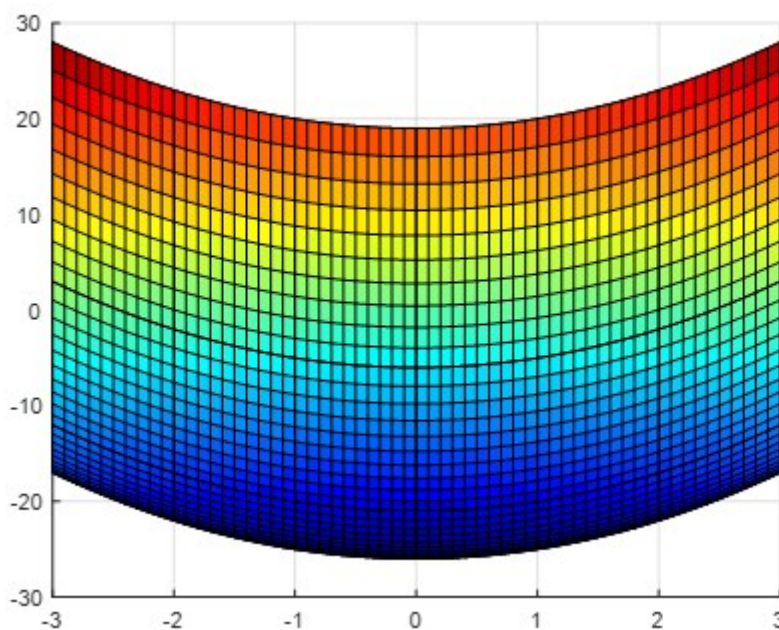


Figure 9:  $\sigma z$  view of Figure 6.

## 5. Conclusion

This study proposes alternate techniques to conserve the monotone, positive and convex shapes of the 3D surface data arranged over a rectangular grid. The developed schemes use  $GC^1$  bi-cubic interpolating function for visualization. Free parameters have been constrained and a range of values on those parameters have been operated to maintain the inherent shape characteristic of data. Here, the suggested shape



preserving interpolating techniques are local,  $GC^1$  and applicable to uniform and non-uniform data. The interpolant used in this paper has a unique degree over the entire domain. The computational cost of the proposed algorithm has also been compared with existing schemes in literature and has been encapsulated in Table 1. The proposed scheme, however, does not use free parameters, which provide users minimal flexibility to change the shape of the data as they desire.

## References

- [1] G. Beliaikov, *Monotonicity preserving approximation of multivariate scattered data*, BIT Numer. Math. **45**(4) (2005), 653-677.
- [2] M. Hussain, M. Z. Hussain, and M. Sarfraz, *Shape-preserving polynomial interpolation scheme*, Iran. J. Sci. Technol. Trans. A: Sci. **40**(1) (2016), 9-18.
- [3] M. Hussain, M. Z. Hussain and A. Waseem,  *$GC^1$  shape preserving trigonometric functions*, Comput. Appl. Math. **33** (2014), 411-431.
- [4] M. Z. Hussain, M. Hussain and B. Aqeel, *Shape -preserving surfaces with constraints on tension parameters*, Appl. Math. Comput. **247** (2014), 442-464.
- [5] M. Z. Hussain and S. Bashir, *Shape-preserving surface data visualization using rational bi-cubic functions*, J. Numer. Math. **19**(4) (2011), 267-307.
- [6] M. Z. Hussain and M. Hussain,  *$C^1$  positive scattered data interpolation*, Comput. Math. with Appl. **59** (2010) , 457-467.
- [7] M. Sarfraz, M. Z. Hussain and M. Hussain, *Modeling rational spline for visualization of shaped data*, J. Numer. Math. **21**(1) (2013), 63-88.
- [8] M. Sarfraz, M. Z. Hussain and M. Hussain, *Shape-preserving curve interpolation*, Int J Comput Math. **89**(1) (2012), 35-53.
- [9] M. Sarfraz and M. Z. Hussain. *Data visualization using rational spline interpolation*, J. Comput. Appl. Math. **189** (2006), 513-525.
- [10] M. Hussain, M. Z. Hussain, A. Waseem and M. Javaid,  *$GC^1$  Shape preserving trigonometric surfaces*, J. Math. Imaging Vis. **53** (2015), 21-41.
- [11] M. Z. Hussain and M. Sarfraz, *Positivity-preserving interpolation of positive data by rational cubics*, J. Comput. Appl. Math. **218** (2008), 446-458. 1
- [12] P. Costantini and C. Manni, *A bicubic shape-preserving blending scheme*, Comput. Aided Geom. Des. **13** (1996), 307-331.
- [13] Q. Duan, F. Bao and Y. Zhang, *Shape control of a bivariate interpolating spline surface*, Int J Comput Math. **85** (5) (2008), 813-825.
- [14] S. Butt and K. W. Brodlie, *Preserving positivity using piecewise cubic interpolation*, Comput Graph. **17**(1) (1993), 55-64.
- [15] S. Butt and K. W. Brodlie, *Preserving convexity using piecewise cubic interpolation*, Comput Graph **15**(1) (1991), 15-23.
- [16] S. Samreen, M. Sarfraz and M. Z. Hussain, *A quadratic trigonometric spline for curve modeling*, PLoS One. **14**(1): e0208015 (2019), <https://doi.org/10.1371/journal.pone.0208015>.
- [17] V. V. Bogdanov and Yu. S. Volkov, *Shape preservation conditions for cubic spline Interpolation*, Sib. Adv. Math. **29** (2019). 231-262.
- [18] S. A. Abdul Karim, *Construction new rational cubic spline with application in shape preservations*, Cogent Eng. **5** (2018), 1505175. <https://doi.org/10.1080/23311916.2018.1505175>
- [19] X. Peng, Z. Li and Q. Sun. *Non-negativity preserving interpolation by  $C^1$  bivariate rational spline surface*, J. Appl. Math. (2012), 1-12.
- [20] X. Han, *Shape-preserving piecewise rational interpolant with quartic numerator and quadratic denominator*, Appl. Math. Comput. **251** (2015), 258-274.